

Clay settling in fresh and salt water

Bruce R. Sutherland · Kai J. Barrett ·
Murray K. Gingras

Received: 28 January 2014 / Accepted: 22 May 2014 / Published online: 20 June 2014
© Springer Science+Business Media Dordrecht 2014

Abstract To gain insight into the process of sedimentation occurring when clay-laden estuaries and deltas enter marine water, we perform laboratory experiments to measure the settling rate of initially unflocculated kaolin clay in fresh and salt water. In fresh water, sedimentation is a slow process with the clay particle concentration gradually decreasing nearly uniformly over hours, consistent with the time-scale expected for particles falling at the Stokes settling speed. The dynamics are dramatically different for clay setting in salt water with salinities between $S = 10$ and 70 psu. Within minutes the clay particles flocculate and a sharp concentration-front between clear water (above) and water with clay in suspension (below) forms near the surface. After formation the concentration-front descends at a near constant speed until the effects of hindered settling become important. When the concentration-front forms in saline fluid, the 10 cm deep tank is cleared of particles in tens of minutes instead of tens of hours as is the case for settling in fresh water ($S = 0$). The initial speed of descent of the front, w , depends weakly upon salinity, S , with virtually no dependence upon S provided $S \gtrsim 20$ psu. However, the descent speed, w , depends strongly upon clay concentration, C , with w decreasing as C increases according to a power law: $w \propto C^{-1.7}$. The results are consistent with observations of relatively quiescent sediment-laden estuaries and deltas where they empty into the ocean.

Keywords Particle settling · Flocculation · Sedimentation

Electronic supplementary material The online version of this article (doi:[10.1007/s10652-014-9365-0](https://doi.org/10.1007/s10652-014-9365-0)) contains supplementary material, which is available to authorized users.

B. R. Sutherland (✉)
Departments of Physics and of Earth & Atmospheric Sciences, University of Alberta,
Edmonton, AB T6G 2E1, Canada
e-mail: bruce.sutherland@ualberta.ca

K. J. Barrett
Department of Physics, University of Alberta, Edmonton, AB, Canada

M. K. Gingras
Department Earth & Atmospheric Sciences, University of Alberta, Edmonton, AB, Canada

1 Introduction

In natural settings, flocculation of clay minerals occurs dominantly in estuaries and deltas where fluvial (i.e., ~ 0 psu) waters are mixed with marine waters (~ 30 psu). This process of sedimentation is of interest as it strongly influences the distribution of fine-grained sediment in these marginal-marine locales. Parameterizing mud-bed sedimentation can help to interpret mud-rock distribution in the stratigraphic record. For example, within estuaries the inner half is more prone to hosting clay-dominated strata. In contrast, deltas export mud to the delta front and prodelta.

Herein we present the results of simple experiments that provide insight into the influence of salinity upon flocculation and settling of clay particles. The experiment results allow us to develop an empirical model characterizing the influence that salinity has on the rate of settling of inorganic particles as a result of changes in the flocculation of the clay mineral kaolinite. We also show that increasing the salinity beyond a nominal value does not change the settling rate, whereas this rate is retarded as particle concentrations become large.

Through a combination of laboratory experiments and observations, several models have been proposed for the deposition (as well as erosion) rate of fines in turbulent shear flow. Generally these assume the deposition rate is proportional to concentration, C , of particles and the settling velocity, w_s [16–18, 21, 24, 26, 34]. Specifically, in the study of Winterwerp [34], the deposition rate was shown to be given simply by their product: $D = w_s C_b$ in which w_s depends upon time but not depth, and C_b is the near-bottom concentration. The laboratory experiments, designed to study the simultaneous processes of deposition and erosion, were performed in flume tanks with particles premixed with saline water. As such they did not focus specifically upon deposition as it depends upon salinity and particle concentration in the absence of turbulent stresses.

Oligohaline (0.5–5 psu) and mesohaline salinities (5–18 psu) are broadly accepted to induce flocculation and clay settling [2, 7, 32]. This corresponds well to studies in modern estuaries, where the turbidity maximum zone is normally positioned within the inner estuary, and where salinities are characteristically below 10 psu [10, 32]. For example, in a study of Chesapeake Bay by Cerco et al. [3] the summertime turbidity maxima for the northern and northeastern estuary reaches occur approximately in the range 7.5–12.5 psu (in the winter, salinity is ~ 5 psu lower in those areas). This is likely a result of enhanced flocculation and tidal resuspension in the area of pronounced flocculation. Suspended sediment content decreases in the seaward direction, which is interpreted to be a result of clay sedimentation in the inner estuary and dilution from sea water. The overall distribution of fine sediment is more complicated, in that some tributaries to Chesapeake Bay (e.g., the Choptank and Nanticoke rivers) contribute little in the way of fine sediment, and thus display no pronounced turbidity maximum. In contrast, the James River is closer to the bay mouth and its associated sediment is deposited further seaward than the other rivers.

Although this qualitative link between salinity and suspended inorganic solids is particularly clear in Chesapeake Bay (Cerco et al. [3], Fig. 5a), it has also been observed in the Gironde Estuary, France [1], the Jiaojiang Estuary, China (Guan et al. [11], Fig. 5), and in Kouchibouguac Bay, Canada [13], to name a few.

Such trends in particle settling and sedimentation may be understood from the chemical behaviour of clay minerals. Individual clay particles are plate shaped with negative charges around their perimeter and positive charges in the center. This arrangement of charges is such that plates repel each other when dispersed in fresh water. However, if the water is saline, sodium and chlorine ions act to neutralize the repulsive forces so that the plates may flocculate. Consequently, clay is expected to settle as flocs in salt water faster than as individual plates in

fresh water. Indeed, clay settling in salt water qualitatively changes the nature of the settling dynamics. When flocs form and settle, they sweep up smaller particles and flocs beneath them as they fall. Thus, the incident flocs grow to larger size and fall faster and more efficiently, sweeping up smaller particles. This positive feedback leads to the formation of a descending concentration-front between near surface fresh water, which has been swept nearly clear of clay, and concentrated clay flocs [5]. The concentration-front should not be confused with the lutocline associated with the rapid increase of clay concentration with depth between suspended clays and the mobile fluid mud layer overlying the sediment bed [25]. Herein, by “concentration-front” we refer to the rapid increase in clay concentration from water devoid of clay near the surface to suspended clay particles below.

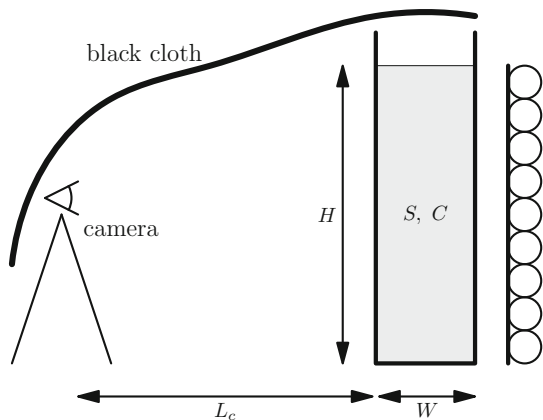
In this study, we perform controlled laboratory experiments to examine the formation of the concentration-front as it depends upon clay concentration and ambient salinity. The experimental set-up and analysis methods are described in Sect. 2. Here we also present qualitative results showing how salinity is responsible for the formation of clay concentration-fronts in mixtures of initially unflocculated clay. In Sect. 3 we quantify for the first time the formation time and rate of descent of the concentration-front as a function of clay concentration and salinity. Connections between this work and observations of enhanced sedimentation at fluvial outflows into the ocean are discussed in Sect. 4.

2 Set-up, analytical methods and qualitative results

The experiment set-up is sketched in Fig. 1. More than 50 experiments were performed in a rectangular tank with 0.5 cm thick acrylic side walls. The interior length and width of the tank is 20.0 and 5.1 cm, respectively. The tank is 30 cm tall, but the tank was filled to 10 (± 0.1) cm with fresh water at the start of an experiment. A specified mass of salt (if any) was then mixed in and the resulting density measured to five-digit accuracy using an Anton Paar DMA 4500 density meter. We performed experiments with saline solutions ranging between fresh and 70 psu.

A specified mass of kaolin clay was then added to the fresh or salt water. Over all, three types of clays were examined. In the experiments for which the formation and evolution of the concentration-front was examined quantitatively, we used K-WHITE 5000, calcined aluminum silicate powder [45 (± 2) % Al_2O_3 and 52 (± 2) % SiO_2] from American Ele-

Fig. 1 Experimental setup showing the side view of the tank filled to depth H with water having salinity S and clay concentration C . A camera (left) looks through the tank, which is lit from behind by a bank of lights (right) diffused by a translucent white plastic sheet. The interior width of the tank is W and the distance from the front of the tank to the camera is L_c



ments. Referred to hereafter as “KW5000 clay”, 90 % of the powder consisted of particles with size near $2\ \mu\text{m}$ with $<0.005\%$ of the particles having size above $\sim 45\ \mu\text{m}$. These particles were chosen because of their good suspension capacity and easy dispersing performance. As we demonstrate below, KW5000 clay showed a clear distinction between settling in fresh water, for which no concentration-front developed, and settling in salt water, for which the concentration-front was well defined and the upper ambient was rapidly cleared of clay particles. We also performed experiments using silty clay (XRD analysis indicates a mixture of illite and kaolinite in unmeasured proportions) collected from the reaches of the Palix River at Willapa Bay (south-west Washington) and using hydrated aluminum silicate kaolin clay from Fisher Scientific (K2-500: $\text{H}_2\text{Al}_2\text{Si}_2\text{O}_8\text{-H}_2\text{O}$). These latter two types of clay were found to settle rapidly (on the order of minutes) whether in fresh or salt water. Presumably this occurred because the clays, having previously been wetted and consolidated, had already formed flocs much larger than individual plates of clay.

In all experiments, the concentration of clay added varied between 15 and 40 ppt by weight. Such concentrations were deemed sufficiently small that particles should fall at least initially without being influenced by surrounding particles. Of course, as the settling particles consolidate near the bottom of the tank, the particle concentration there would increase and the settling of each particle would be hindered by the ambient flow moving upward around the neighbouring particles [19,22,30,33]. However, the study here is concerned more with the initial progression of clay concentration-fronts that develop in saline water well above the sediment bed. There the clay concentration is small but, due to flocculation, the effective particle size should increase, thus increasing the settling speed and thereby establishing a clay concentration-front.

The KW5000 clay powder was added to the water in the tank while being stirred vigorously with a mixer until the mixture was uniform. The stirrer was then extracted and this was taken to be the start time ($t = 0$) of most experiments. To examine the effect of particle consolidation and possible de-gassing of the particles, in some experiments we allowed the clay to settle overnight and then re-stirred the mixture.

To visualize the evolution of the flow, either a halogen light or a bank of fluorescent bulbs was placed well behind the tank and, to diffuse the lighting, a translucent white plastic sheet was placed against the back of the tank extending from the bottom to 10 cm height. Above this, black construction paper was fastened between 10 cm and the top of the tank. Finally, a black cloth was draped over the setup between the camera lens and the tank. In this way, the only light that reached the camera passed through the mixture in the tank.

Experiments were recorded on a Sony Digital CCD camcorder or a Panasonic HDC-HS250 digital camcorder. The shutter speed and iris were fixed so that the light intensity reaching the camera qualitatively measured the concentration of clay in the solution: low intensity indicated high light attenuation resulting from relatively high clay concentration; high intensity indicated relatively low clay concentration. The camera was placed 1.5 m from the front of the tank with its field of view spanning the height and most of the tank width.

Figure 2 shows snapshots and vertical time series constructed from four experiments with KW5000 clay settling in fresh and salt water. In Fig. 2a, clay added to fresh water remained well suspended even after 25 min. This is apparent because the intensity of light passing through the tank hardly changed over time from top to bottom. Experiments of this circumstance run for long times showed that it took over 10 h before all the clay had settled to the bottom 1 cm of the tank. This is consistent with the settling time predicted for individual spherical particles of radius $r_p = 1\ \mu\text{m}$ and density $\rho_p = 2\ \text{g/cm}^3$ to fall $H = 10\ \text{cm}$ at the Stokes settling velocity,

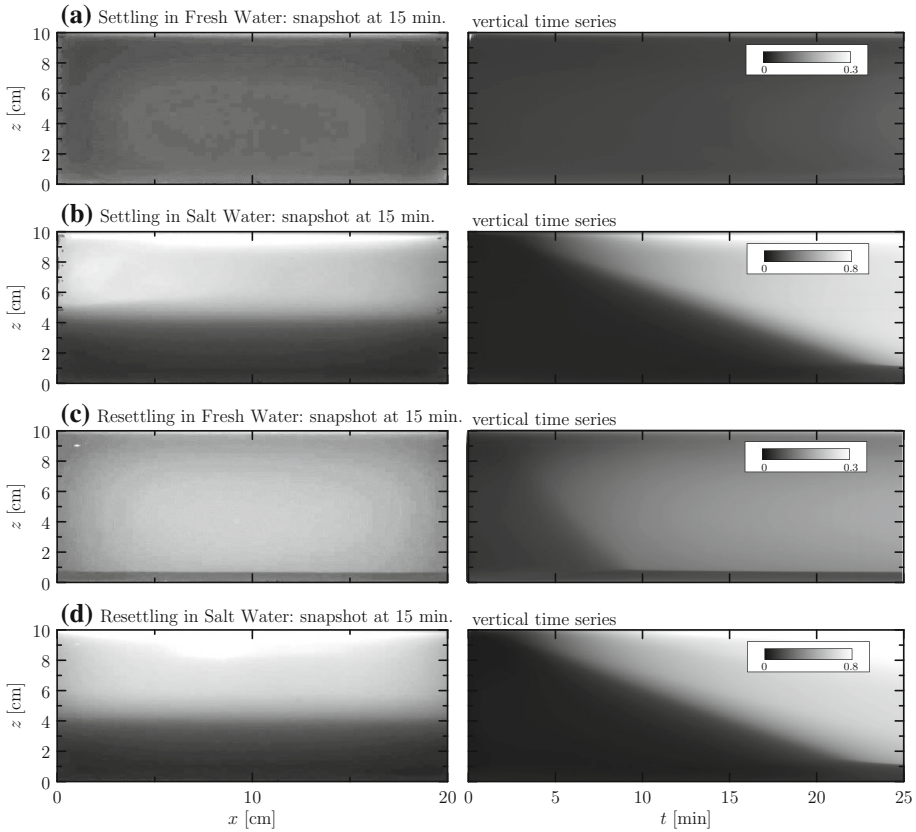


Fig. 2 Snapshots after 15 min (*left column*) and vertical time series of along-tank-averaged light intensity (*right column*) taken from experiments with 14.7 ppt KW5000 clay settling in fresh and salt water: **a** dry clay mixed with fresh water, **b** dry clay mixed with 5 psu saline water (11.0g NaCl added to tank), **c** clay in fresh water settles 20 h and is then remixed before start of experiment, **d** after this experiment, 11.0g NaCl added to tank and the 5 psu saline water is mixed with resuspended clay before start of experiment. The *gray scale* for intensity in each snapshot and corresponding time series is indicated in the *top-right* of each time series plot. Note the intensity of light passing through the tank is significantly brighter near the surface in the salt-water experiments (time-lapse movies of these experiments can be viewed as supplemental material)

$$w_s = \frac{2}{9} \frac{g' r_p^2}{\nu}, \tag{1}$$

in which $g' = g(\rho_p - \rho_w)/\rho_w$ is the reduced gravity, and $\rho_w = 0.9982 \text{ g/cm}^3$ and $\nu = 0.01 \text{ cm}^2/\text{s}$ are respectively the density and kinematic viscosity of fresh water at room temperature. Explicitly, we estimate $w_s \simeq 2 \times 10^{-4} \text{ cm/s}$, which gives a setting time of $H/w_s = 5 \times 10^4 \text{ s} \simeq 13 \text{ h}$.

In contrast, Fig. 2b shows the development of a well-defined clay concentration-front when clay settles in salt water. After 15 min the front was situated at mid-depth with virtually no particles in suspension near the surface where the intensity of light passing through the tank was bright, and a high concentration of particles near the bottom where the intensity of light was dark. The vertical time series to the right shows the concentration-front developed after about 5 min and then descended at a constant speed for ~ 20 min. After this time the clay

consolidated sufficiently near the tank bottom so that settling was hindered and the advance of the concentration-front slowed.

Comparing these two experiments clearly shows that salinity results in the development of a clay concentration-front, which significantly enhances the speed at which the particles settle. Even in the absence of salinity, clay may settle quickly if the particles have already flocculated. This was observed in experiments using Fisher K2-500 clay and with clay gathered from Willapa Bay. Some evidence of this was also seen in experiments with KW5000 clay. Figure 2c shows the results of an experiment in which KW5000 clay was allowed to settle overnight in fresh water before being remixed. Unlike the experiment shown in 3a, here a fraction of the particles are observed to settle out in the first 10 min of the experiment. Presumably, these were particles that formed flocs while consolidating at the bottom of the tank. However, a substantial fraction of the clay particles remained in suspension even after 25 min, as evident by the relatively low intensity of light passing through the tank even near the surface (note that the intensity scale ranges from 0 to 0.3 in Fig. 2c whereas it ranges from 0 to 0.8 in Fig. 2b).

When the same amount of salt was added to the tank as was added in the experiment shown in Fig. 2b, we observe once again the formation of a clay concentration-front that separated particle-free fluid near the surface from high particle concentrations near the base (Fig. 2d).

Thus clay may settle quickly in fresh water if it has already undergone processes that permit the formation of large flocs [27]. But if the clay suspension remains fine (with particle sizes on the order of 1 μm), salinity clearly acts as a catalyst to the formation of flocs while the clay is still in suspension.

This paper seeks to quantify the development and evolution of the clay concentration-fronts sufficiently far above the sediment bed where hindered settling plays an insignificant role. To track the front position in time, we sequentially examined frames from movies of the experiment. Each frame was imported into the image- and data-analysis software “MatLab” (www.mathworks.com) where the digitized intensities were represented by a matrix from which we calculated the horizontally averaged intensity as a function of height. Concatenating this time-dependent data, with a resolution of 1 s, we constructed vertical time series.

Figure 3 shows vertical time series constructed from the results of four experiments examining the settling of KW5000 clay in ambient with different salinities. These illustrate a qualitative difference in behaviour for clay setting in fresh and saline water. For clay in fresh water, the system remained well mixed while the overall concentration slowly decreased (Fig. 3a). In most experiments, clay was still partially in suspension after being left overnight. However, if the ambient water was moderately saline, a front was developed where the concentration of clay rapidly decreased with height. This front descended relatively rapidly, so that most of the clay had fallen out of suspension within an hour. In cases with low salinity, the front took longer to develop, but then descended rapidly (Fig. 3b). In experiments with greater salinity, the front formed relatively quickly and was relatively sharp, exhibiting a 50 % intensity change from dark to light (from high to low clay concentration) over less than a centimeter height (Fig. 3c). The front was found to develop and descend most quickly if the clay concentrations were low in sufficiently salty water. In such cases, however, the front was not so sharply defined (Fig. 3d).

To provide a quantitative measure of these observations, we characterized the formation time and descent of the front by superimposing contours of constant intensity on the vertical time series and determining the best-fit line over a fixed vertical range, as illustrated in Fig. 4. We then found the minimum and maximum intensities, I_{\min} and I_{\max} , respectively. From these we computed the low, intermediate and high intensities given respectively by

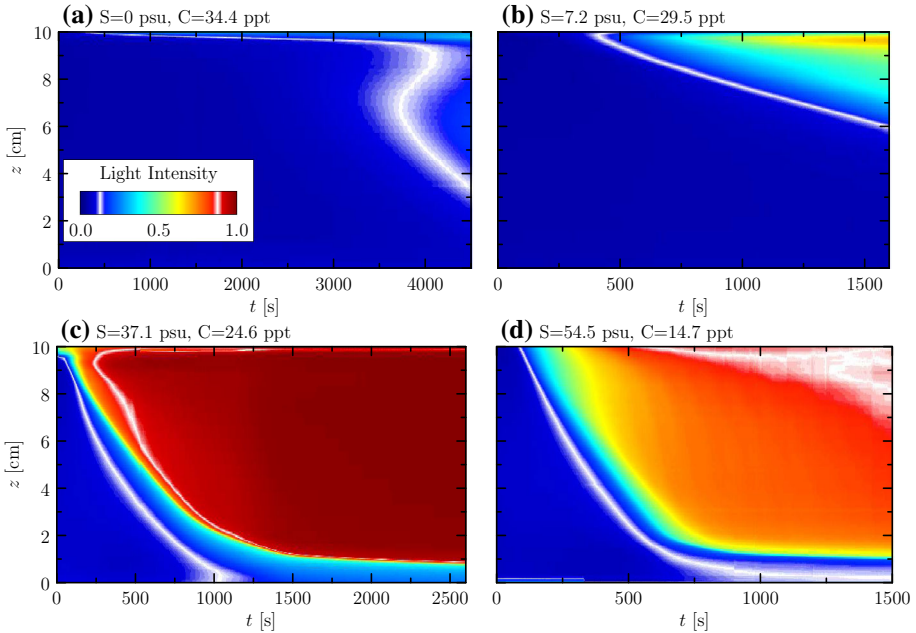


Fig. 3 Vertical time series showing in *false-color* (inset to **a**) the average intensity of light reaching the camera over time between the bottom and surface of the solution in the tank in four experiments with **a** zero salinity, **b** low salinity and high clay concentration, **c** high salinity and high clay concentration and **d** high salinity and low clay concentration. Light intensities near zero indicate high clay concentration whereas high intensities, near one, indicate low clay concentrations. Above each time series are indicated values of salinity (*S*, in practical salinity units) and clay concentration (*C*, in parts solute per thousand parts water by mass). All experiments are performed with KW5000 clay

$$\begin{aligned}
 I_1 &= \frac{3}{4}I_{\min} + \frac{1}{4}I_{\max} \\
 I_2 &= \frac{1}{2}I_{\min} + \frac{1}{2}I_{\max} \\
 I_3 &= \frac{1}{4}I_{\min} + \frac{3}{4}I_{\max}.
 \end{aligned}
 \tag{2}$$

In the analysis of most experiments, the best-fit line to each of the three contours were determined over the range $7\text{ cm} \leq z \leq 8\text{ cm}$. This range was chosen somewhat arbitrarily as the descent speed was observed to be nearly constant until the particles consolidated over the bottom 2 cm of the tank. Although one might expect the concentration-front speed to increase as the flocs in the front to increase in size, apparently any larger flocs fall below away from the concentration front. As such the concentration front represents the transition between ambient fluid which is cleared of particles and fluid containing the smallest flocs.

The formulae for the lines giving the contour height *z* as a function of time *t* were cast in the form

$$z = H - w_i(t - T_{0i}),
 \tag{3}$$

in which *i* = 1, 2 and 3, corresponding to contours with intensity *I*₁, *I*₂ and *I*₃, respectively. The average of the three values of *w*_{*i*} was used as a measure of the settling rate:

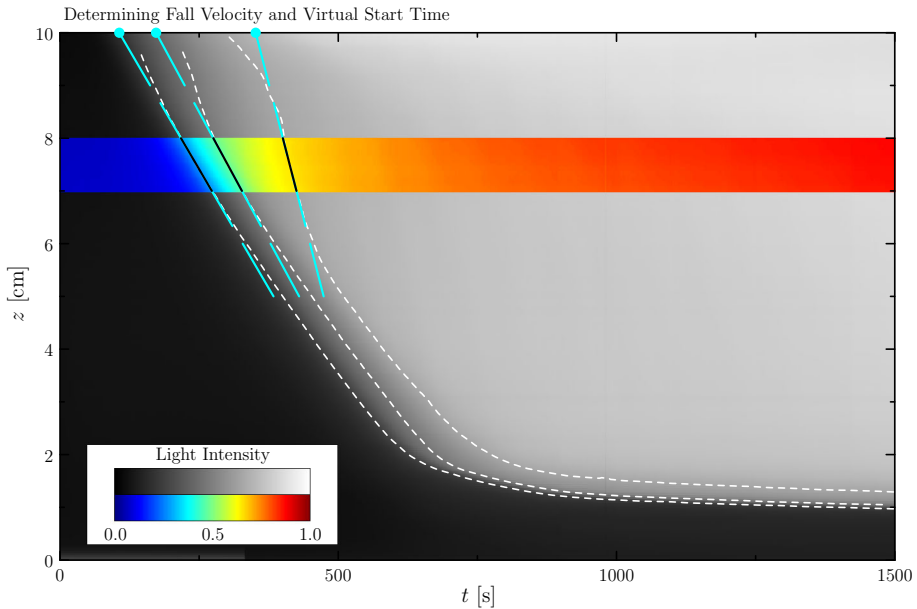


Fig. 4 Determination of the front descent rate and the virtual start time of the descent. The vertical time series shown in Fig. 3d is reproduced as a *gray scale* image of intensity except in the band between $z = 7$ and 8 cm, where a *false-color* intensity scale is used as shown in the inset. *White dashed lines* are drawn along contours of constant intensity $0.28, 0.47,$ and 0.66 . *Solid black lines* in the *color band* show the lines best-fit between $z = 7$ and 8 cm. These are extended as *cyan-dashed lines* to the surface at $z = H = 10$ cm where the virtual start times are defined, as indicated by the three *cyan-colored circles*

$$w = \frac{1}{3}(w_1 + w_2 + w_3). \tag{4}$$

The standard deviation of the three values of w_i gave the error estimate. In experiments with sharp fronts (e.g. Fig. 3c) the error is expected to be small because the three contours would be closely packed together.

As well as measure the front speed, we also estimated the front formation and settling time, as illustrated in Fig. 4. The extrapolation of the three best-fit lines to the surface, where $z = H = 10$ cm, gives the virtual times, T_{0i} , at which the front would have begun to descend had it developed immediately and fallen at the measured settling rate. As in (4), the average and standard deviation of the three values of T_{0i} give the virtual start time T_0 and its error. From the mean settling speed given by (4), the minimum total settling time is estimated to be

$$T_f = T_0 + H/w. \tag{5}$$

Errors in T_f are determined by the corresponding errors in w and T_0 .

In our analysis, we found best-fit lines for z in the range between 7 and 8 cm in all experiments except those with very low salinities ($S \leq 10$ psu). In these cases, a clearly defined front was not evident for long times, and only began to clearly manifest itself at lower depths. In these cases we applied the analysis procedure described above for $6 \leq z \leq 7$ cm.

3 Quantitative results

In all experiments with fresh water and KW5000 clay, no front developed. Rather the concentration of clay gradually decreased in time, while exhibiting little variation in space. Even after more than 10 h, a substantial concentration of clay particles remained in suspension.

In salt water a front between high and low concentrations of clay developed. Our analyses of the formation and evolution of the fronts as a function of ambient salinity, provide insight into the behaviour of clay suspensions in a range of salinities.

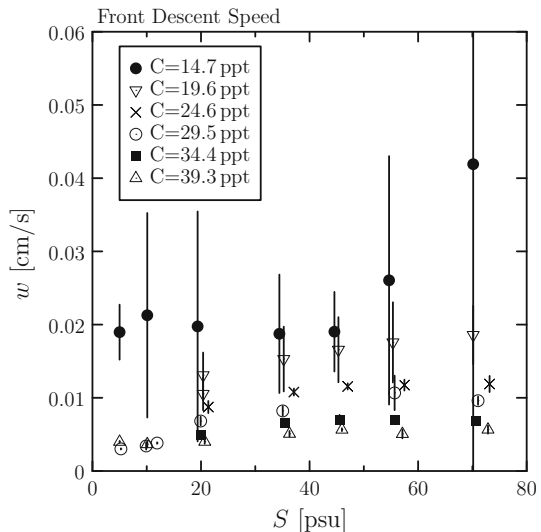
The speed of descent of the front was measured in experiments with different ambient salinities, S , measured in grams of salt per kilogram fresh water [values for which are expressed in practical salinity units (psu), effectively the same as units of parts per thousand (ppt)]. As shown in Fig. 5, at a fixed clay concentration, the speed of descent of the front changes little with salinity provided $S \gtrsim 10$ psu. Hence the clay concentration is the most important factor in determining the front descent rate assuming that the ambient is saline enough for the front to develop at all.

The errors in speed measurement are large for experiments with low concentrations of clay, but are negligible for $C \gtrsim 25$ ppt. Thus, although the front descends quickly if $C = 14.7$ ppt, it is more diffuse than the front in experiments with higher clay concentrations, which is consistent with the time series shown in Figs. 3d and 4.

From the intercepts of the best-fit lines with the surface at $z = H = 10$ cm, we determine the average virtual start time for the front descent. The results in Fig. 6a show that, if the salinity is sufficiently large ($S \gtrsim 10$ psu), and the concentration sufficiently high ($C \gtrsim 25$ ppt), the front forms almost immediately when the experiment begins. If the clay concentration is lower, the front takes longer to develop and, as indicated by the error estimates, it is more diffuse.

Significantly, if the salinity is low ($S \lesssim 10$ psu), the time for development of the front takes tens of minutes. The front itself is quite diffuse having errors in the virtual start time on the order of hundreds of seconds.

Fig. 5 Measured speed of descent of the concentration-front, w , as a function of salinity, S . Different symbols correspond to different clay concentrations as indicated in the legend. Points are drawn at the mean value with vertical lines indicating the size of error estimates



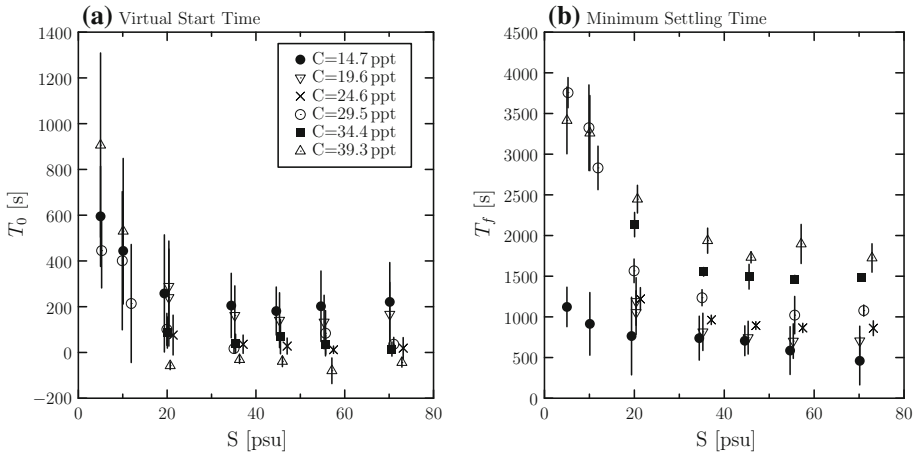


Fig. 6 **a** Virtual start time of front descent, T_0 and **b** linearly extrapolated time for complete settling, T_f . Both are plotted as a function of salinity, S , with clay concentrations, C , for both T_0 and T_f plots shown in the inset of **a**)

An estimate of the minimum settling time was computed using (5). The results are plotted in Fig. 6b. The fastest settling times (~ 10 min) occurred in solutions with low clay concentrations ($C \lesssim 20$ ppt) in moderately saline fluid ($S \gtrsim 10$ psu). The settling time increased as the clay concentration increased because the front descent rate was smaller, even though the front took less time to develop. In ambient water with low salinity, the settling time was very long because the front descended slowly and took a long time to develop. In the limit of zero salinity, the front did not develop at all and setting was a long process.

In an attempt to synthesize these results we analyzed the descent rate as a function of clay concentration (Fig. 7). The mean descent speed is the average, \bar{w} , of the speeds measured in experiments with fixed clay concentration and salinities ranging between 20 and 60 psu. Generally, we found that the front speed decreased as the concentration increased. When plotted on log-log axes (Fig. 7, inset), the curve forms a straight line with slope -1.7 . This gives an empirical measurement for the front descent rate of

$$\bar{w} = W_0(C/C_0)^{-1.7}, \tag{6}$$

in which, somewhat arbitrarily, we have set the coefficients for the case $C_0 = 40$ ppt for which $W_0 = 0.005$ cm/s.

4 Discussion and conclusions

The experimental results shed light on 3 aspects of mud sedimentation. First, they confirm and help parameterize the observation that clay readily flocculates at low salinities that are coincidental with salinity distributions in estuaries. In general, our lab results are in accordance with studies of modern estuaries [1, 11, 13], which suggest that in these natural settings, most clay flocculation occurs at salinities near 10 psu.

The dependence of settling rate on clay concentration helps to explain sedimentation that leads to the accumulation of inclined heterolithic stratification (IHS), which is commonly associated with inner estuary and distributary channel settings [4, 15, 29]. IHS consists of

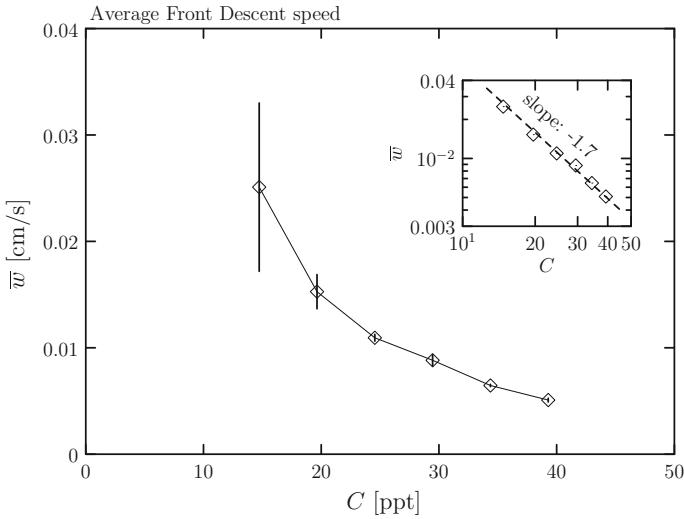


Fig. 7 Mean speed of front descent, \bar{w} , as a function of clay concentration. The mean speed is computed by averaging the speeds w measured in experiments with fixed clay concentration and with salinities between 20 and 80 psu. The inset shows a plot of the same data on log-log axes. The best-fit line through the points plotted against these axes is indicated by the dashed line in the inset

interbedded mud and sand, and they are normally ascribed to seasonal variations in estuary sedimentation. Nominally, the sand beds are taken to indicate high volumes of fluvial discharge with the mud-beds indicating low fluvial flux. Our results suggest that mud sedimentation is substantially slowed with increased clay concentration (Figs. 5, 7). As such, when clay concentration in the fluvial waters increases (e.g. during a riverine flood), the estuary mud plume can extend much further seaward. As such, associating mud distribution to depositional energy or to the location of the saline-fresh water mixing zone is not necessarily cogent. The corollary to this is that the influence of suspended clay concentration should additionally be considered in the interpretation of mud sedimentation in landward versus seaward parts of the estuary. If strong currents and turbulent processes do not play dominant roles, then in the inner estuary mud-bed deposition reflects times when mud concentration is low and changes in salinity effectively flocculate clay and promote settling. Mud beds in more seaward parts of the estuary result from episodes of greater clay concentration whose settling front speed is slower even in relatively quiescent fluid with concentrations as low as 40 ppt. Because of this and the additional affects of turbulent mixing, the mud-plume can far exceed the zone of salt- and fresh-water mixing.

Second, the data indicate that salinities above 10 psu do not increasingly promote sedimentation, suggesting that sediment-distribution patterns in higher salinity basins will be similar to those observed in estuaries. The observation that settling rates are not noticeably increased in water that exceeds 20 psu (Fig. 5) suggests that where sediment is delivered to marine basins, as in a delta, the resulting sediment plume, which is an important mechanism for delivering sediment to the shelf, can interact substantially with marine waters before forming large flocs. This may explain the longevity of large sediment plumes. The Amazon Shelf, for example, receives sediment at distances greater than 1,400 km from the Amazon River Mouth [9]. In this case, the large volume of river discharge produces a low-saline surface layer, the basal salinity front of which is controlled by tidal mixing. The resulting plume is generally 5–10 m thick, with a salinity of 20–30 psu [8]. If increasing salinities resulted

in ever increasing flocculation rates, such delta plumes would rapidly lose clay sediment and offshore sediment transport would be greatly reduced.

A third important conclusion of this study is that high sediment concentrations discourage flocculation and may offer another mechanism for modeling offshore sediment transport in both hyperpycnal and hypopycnal plumes. Specifically, we show that there is a tendency for settling rates to slow where the suspended-sediment load exceeds 10 g/L. In most estuary settings suspended sediment ranges in the turbidity maximum zone fall well below this threshold. Many tributaries of Chesapeake Bay, as well as Willapa Bay, Tillamook Bay and Coos Bay (west coast USA), display ~ 1 g/L suspended sediment in the inner estuary [31]. There are exceptions: the Amazon River estuary approaches 10 g/L [8]; the Changjiang Estuary, China ranges from 0.5 to 10 g/L [28]; the Fly River delta in Papua New Guinea has a turbidity maximum of 10 g/L [12]; the Trent Estuary in the UK reaches ~ 12 g/L [23]; and the Gironde Estuary locally exceeds 12 g/L [6]. All of the high-suspended-sediment-load examples cited above export fine sediment to the oceanic basin, whereas estuaries with low fine-grained sediment concentration discharge normally do not. This suggests that under conditions of high suspended-sediment loads, interference in the flocculation process is at least a factor in transporting clay to the ocean basin.

The impairment of flocculation due to high suspended-sediment concentration may also be a factor in delivering fluid muds to the shelf. Fluid mud deposits are increasingly identified in the rock record, and are broadly ascribed to delta-associated density currents comprising sediment-laden hyperpycnal flows derived from high-volume river discharge. Resulting density flows can travel long distances [20], and are thought to represent an important process in transporting mud to the shelf. In recent observations of hyperpycnal flows, the suspended sediment load exceeds 7 g/L (e.g., Waipaoa, NZ, 28 g/L [14]; the Fly River, PNG, 10 g/L [12]). Although speculative, based on the data, it is reasonable to hypothesize that the coherence of fluid muds may be in part maintained by the diminished flocculation rate of clay in the marine basin.

Being performed in a stationary ambient fluid, our experiments neglect the ambient flow dynamics of estuaries, deltas and river plumes including the influence of turbulence, waves, currents, tides and motion near complex topography. As such our results are strictly applicable to relatively quiescent flows far from the influence of turbulence resulting from wind stress and breaking waves in the surface mixed layer and from breaking internal waves and boundary layer processes. The next stage of research will examine the influence of turbulence in enhancing or disrupting flocculation and the formation of the concentration front.

Most of the experiments reported upon here used a synthetic clay, KW5000. This clay was useful for the purposes of running controlled laboratory experiments because the microscopic platelets of this clay were not significantly flocculated in dry form and because they readily dispersed without flocculating when first mixed into fresh water. Future work will examine sedimentation of clays extracted from river estuaries with an aim of understanding the influence of sea water upon pre-consolidated clay.

Acknowledgments This research was supported by the National Science and Engineering Research Council of Canada (NSERC).

References

1. Allen GP, Posamentier HW (1993) Sequence stratigraphy and facies model of an incised valley fill; the Gironde Estuary, France. *J Sediment Petrol* 63(3):378–391

2. Ani SA, Dyer KR, Huntley DA (1991) Measurement of the influence of salinity on flocculation and strength. *Geo-Mar Lett* 11:154–158
3. Cerco CF, Kim SC, Noel MR (2013) Management modeling of suspended solids in the Chesapeake Bay, USA. *Estuar Coast Shelf Sci* 116:87–98
4. Choi K (2010) Rhythmic climbing-ripple cross-lamination in inclined heterolithic stratification (IHS) of a macrotidal estuarine channel, Gomso Bay, west coast of Korea. *J Sediment Res* 80(6):550–561
5. Couch MC, Hinch EJ (1991) Sedimentation, aggregation and compaction. In: Bideau D, Dodds JA (eds) *Physics of Granular Media*. Nova Sciences, New York, pp 299–321
6. Doxaran D, Froidefond JM, Castaing P, Babin M (2009) Dynamics of the turbidity maximum zone in a macrotidal estuary (the Gironde, France): observations from field and MODIS satellite data. *Estuar Coast Shelf Sci* 81(3):321–332
7. Eisma D, Cadée GC (1991) Particulate matter processes in estuaries. *SCOPE* 42:283–296
8. Geyer WR, Beardsley RC, Lentz SJ, Candela J, Limeburner R, Johns WE, Soares ID (1996) Physical oceanography of the Amazon shelf. *Cont Shelf Res* 16(5–6):575–616
9. Gibbs RJ (1977) Clay mineral segregation in the marine environment. *J Sediment Petrol* 47(1):237–243
10. Gingras MK, Pemberton SG, Saunders T, Clifton HE (1999) The ichnology of modern and pleistocene brackish-water deposits at Willapa Bay, Washington; variability in estuarine settings. *Palaios* 14(4):352–374
11. Guan WB, Kot SC, Wolanski E (2005) 3-D fluid-mud dynamics in the Jiaojiang Estuary, China. *Estuar Coast Shelf Sci* 65(4):747–762
12. Harris PT, Hughes MG, Baker EK, Dalrymple RW, Keene JB (2004) Sediment transport in distributary channels and its export to pro-deltaic environment in a tidally dominated delta: fly river, Papua New Guinea. *Cont Shelf Res* 24:2431–2454
13. Hauck TE, Dashtgard SE, Pemberton SG, Gingras MK (2009) Brackish-water ichnological trends in a microtidal barrier island-embayment system, Kouchibouguac National Park, New Brunswick, Canada. *Palaios* 24(8):478–496
14. Hicks DM, Gomez B, Trustrum NA (2004) Event suspended sediment characteristics and the generation of hyperpycnal plumes at river mouths: East coast continental margin, north island, New Zealand. *J Geol* 112:471–485
15. Hovikoski J, Rasanen M, Gingras MK, Ranzi A, Melo J (2008) Tidal and seasonal controls in the formation of late Miocene inclined heterolithic stratification deposits, western Amazonian foreland basin. *Sedimentology* 55(3):499–530
16. Khelifa A, Hill PS (2006) Models for effective density and settling velocity of flocs. *J Hydraul Res* 44(3):390–401
17. Krone RB (1962) Flume studies of the transport of sediment in estuarial shoaling processes. Tech. Rep. Final Report, Hydraulic Engineering Laboratory and Sanitary Engineering Research Laboratory, University of California, Berkeley
18. Krone RB (1993) Sedimentation revisited. In: Mehta AJ (ed) *Nearshore and Estuarine Cohesive Sediment Transport, Coastal and Estuarine Studies*. American Geophysical Union, pp 108–125
19. Kynch G (1952) A theory of sedimentation. *Trans Faraday Soc* 48:166–176
20. Lamb MP, Mohrig D (2009) Do hyperpycnal-flow deposits record river flood dynamics. *Geology* 37(12):1067–1070
21. Lau YI, Krishnappan BB (1994) Does re-entrainment occur during cohesive sediment settling? *J Hydraul Eng* 120(2):236–244
22. Mehta AJ (1986) Characterization of cohesive sediment properties and transport processes in estuaries. In: Mehta AJ (ed) *Estuarine Cohesive Sediment Dynamics*, vol 14, *Lecture Notes in Coastal and Estuarine Studies*. Springer, Berlin, pp 290–325
23. Mitchell SB, Lawler DM, West JR, Couperthwaite JS (2003) Use of continuous turbidity sensor in the prediction of fine sediment transport in the turbidity maximum of the Trent Estuary, UK. *Estuar Coast Shelf Sci* 58:645–652
24. Parchure TM, Mehta AJ (1985) Erosion of soft cohesive sediment deposits. *J Hydraul Eng* 111(10):1308–1326
25. Ross MR, Mehta AJ (1989) On the mechanics of lutoclines and fluid mud. *J Coast Res* 5:51–62
26. Sanford LP, Halka JP (1993) Assessing the paradigm of mutually exclusive erosion and deposition of mud with examples from upper Chesapeake Bay. *Mar Geol* 114:37–57
27. Schieber J, Southard J, Thaisen K (2007) Accretion of mudstone beds from migrating floccule ripples. *Science* 318:1760–1763
28. Shi Z, Kirby R (2003) Observations of fine suspended sediment processes in the turbidity maximum at the north passage of the Changjiang Estuary, China. *J Coast Res* 19(3):529–540

29. Sisulak C, Dashtgard S (2012) Seasonal controls on the development and character of inclined heterolithic stratification in a tide-influenced, fluvially dominated channel; Fraser River, Canada. *J Sediment Res* 82(4):244–257
30. Travkovski P, Wiberg PL, Geyer WR (2007) Observations and modeling of wave-supported sediment gravity flows on the Po prodelta and comparison to prior observations from the Eel Shelf. *Cont Shelf Res* 27:375–399
31. Uncles RJ, Smith RE (2005) A note on the comparative turbidity of some estuaries of the americas. *J Coast Res* 21(4):845–852
32. Uncles RJ, Stephens JA, Law DJ (2006) Turbidity maximum in the macrotidal, highly turbid Humber Estuary, UK; flocs, fluid mud, stationary suspensions and tidal bores. *Estuari Coast Shelf Sci* 67(1–2):30–52
33. Winterwerp JC (2002) On the flocculation and settling velocity of estuarine mud. *Cont Shelf Res* 22:1339–1360
34. Winterwerp JC (2007) On the sedimentation rate of cohesive sediment. In: Maa JPY, Sanford LP, Schoellhamer DH (eds) *Estuarine and coastal fine sediment dynamics*. Elsevier, Amsterdam, pp 209–226